Catal Lett
DOI 10.1007/s10562-016-1889-0

Ruthenium Salen Complex Immobilized on $FeNi_3$ Magnetic Nanoparticles: The Efficient, Green and Reusable Nanocatalyst for Heck and Suzuki Coupling Reactions

Seyed Mohsen Sadeghzadeh[1]

Received: 27 July 2016 / Accepted: 7 October 2016

Abstract $FeNi_3$ as a new magnetic nanoparticles supported ruthenium salencomplex ($FeNi_3/SiO_2$/Salen/Ru MNPs) was successfully prepared by attaching ruthenium acetates to a novel *N,N´*-bis(salicylidine)ethylenediamine ligand functionalized $FeNi_3$. The as-prepared catalyst was characterized by N_2 sorption, UV–vis, TGA, XRD, FTIR, VSM, and TEM. It was found to be an efficient catalyst for Heck and Suzuki coupling reactions in aqueous medium. High catalytic activity and ease of recovery from the reaction mixture using external magnet, and several reuse times without significant losses in performance are additional eco-friendly attributes of this catalytic system.

Graphical Abstract

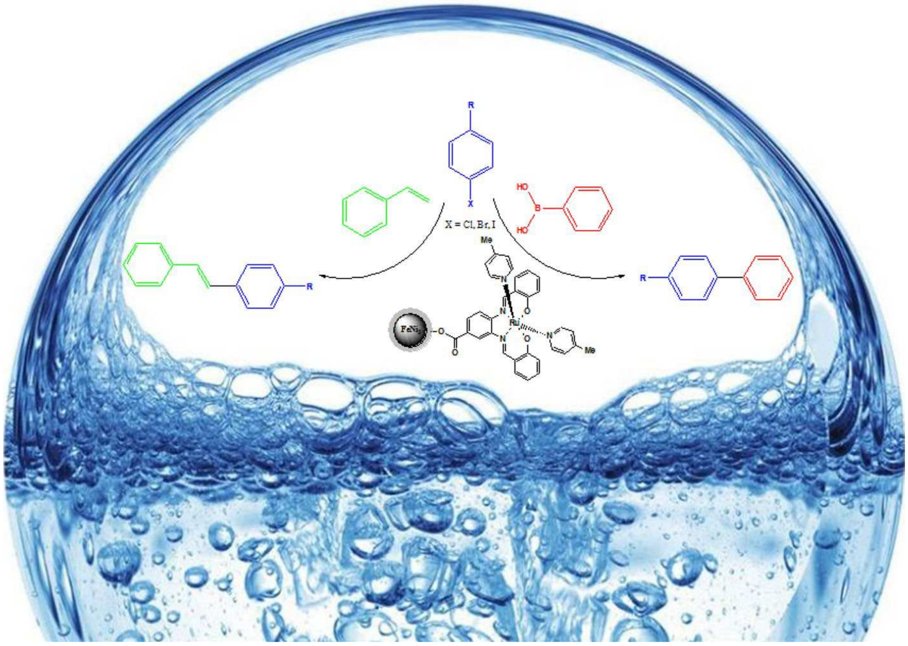

✉ Seyed Mohsen Sadeghzadeh
seyedmohsen.sadeghzadeh@gmail.com

[1] Department of Chemistry, Payame Noor University, Torbat heydarieh, Iran

Keywords Salen · Nanocatalyst · Heck coupling · Suzuki coupling · Green chemistry · Solvent free

1 Introduction

In recent years, magnetic nanoparticles (MNPs), because of providing greater accessibility of active sites for reaction and thereby, enhancing dramatically the contact between reactants and catalyst and also unique features including good stability, easy synthesis and functionalization, high surface area as well as low toxicity and price have emerged as attractive support for the immobilization of homogeneous catalysts [1, 2]. In this regard, $FeNi_3$ MNPs as the catalyst supports, have been attracted more attentions as they can be easily recovered from the reaction mixture, simply by using an external magnet [3–5]. We use $FeNi_3$ instead of Fe_3O_4 as a conventional magnetic core, because Fe_3O_4 MNPs are not highly stable and they may lose their magnetic properties, especially in acidic environments. It must be pointed that there are many concerns on the fact that Fe nanoparticles have fate and transport and the corresponding risks; where as Ni nanoparticles represents a well-known problem for allergy and dermatitis [6–9], but to date has not been published reports of harmful $FeNi_3$.

Transition metal-catalyzed carbon–carbon and carbon-heteroatom bond forming reactions [10] are powerful tools for advanced organic synthesis in both academic [11] and industrial laboratories [12]. In this area, The Heck and Suzuki coupling reaction provides a powerful and straight forward method for C–C bond formation, which has been widely applied to diverse areas such as natural product synthesis, pharmaceuticals, biologically active molecules, and materials science [13–21].

Engaged in the development of greener and sustainable pathways for organic transformations, nanomaterial, and nano-catalysis [22–30], herein, we report a simple and efficient synthesis of a nano-ferrite-supported, magnetically recyclable, and inexpensive ruthenium catalyst and its application for Heck and Suzuki coupling reactions (Scheme1).

2 Experimental

2.1 Materials and Methods

Chemical materials were purchased from Fluka and Merck in high purity. Melting points were determined in open capillaries using an Electrothermal 9100 apparatus are uncorrected. FTIR spectra was recorded on a VERTEX 70 spectrometer (Bruker) in the transmission modein spectroscopic grade KBr pellets for all the powders. Morphology was analyzed transmission electron microscopy (TEM) on a CM_{120} Philips Holland transmission electron microscope operating at 120 kV. The content of phosphorous in the catalyst was determined by OPTIMA 7300DV inductively coupled plasma (ICP) analyzer. Powder X-ray diffraction data was obtained using Bruker D8 Advance model with Cu ka radition. The thermogravimetric analysis (TGA) was carried out on a NETZSCH STA449F3 at a heating rate of $10\,°C\ min^{-1}$ under nitrogen. The magnetic measurement was carried out in a vibrating sample magnetometer (VSM) (4 inch, Daghigh Meghnatis Kashan Co., Kashan, Iran) at room temperature. NMR spectra was recorded in $CDCl_3$ on a Bruker Avance DRX-400 MHz instrument spectrometer using TMS as internal standard. The purity determination of the products and reaction monitoring was accomplished by TLC on silica gel polygram SILG/UV 254 plates.

2.2 General Procedure for the Preparation of $FeNi_3$ Nanoparticles

$FeCl_2·4H_2O$ (1.72 g) and $NiCl_2·6H_2O$ (4.72 g) was dissolved in 80 ml of deaerated highly purified water contained in a three neck flask with vigorous stirring (800 rpm) under nitrogen. As the temperature was elevated to 80 °C, 10 ml of ammonium hydroxide was added drop by drop, and the reaction was maintained for 30 min. hydrazine hydrate (20 ml, 80 % concentration) was added to the above suspension. The black product was separated by putting the vessel on a permanent magnet and the supernatant was decanted. The black precipitate was washed for six times with highly purified water to remove the unreacted chemicals, then the black product $FeNi_3$ was dried in the vacuum.

2.3 General Procedure for the Preparation of $FeNi_3/SiO_2$ Nanoparticles

Firstly, a mixture of ethanol (100 ml) and distilled water (20 ml) was added to magnetic nanoparticles (1 g), and the resulting dispersion was sonicated for 10 min. After adding ammonia water (2.5 ml), tetraethyl orthosilicate (TEOS, 2 ml) was added to the reaction solution. The resulting dispersion was under mechanically stirred continuously for 20 h at room temperature. The magnetic $FeNi_3/SiO_2$ nanoparticles were collected by magnetic separation and washed with ethanol and deionized water in sequence.

2.4 General Procedure for the Preparation of Compound (A) Nanoparticles

For Synthesis of compound (A) MNP (Fig. 1), 2 mmol of $FeNi_3/SiO_2$ MNPs were dispersed in a mixture of 80 ml of ethanol, 20 ml of deioned water and 2.0 ml of 28 wt% concentrated ammonia aqueous solution ($NH_3·H_2O$), followed by the addition of 20 mmol of ethyl 3,4-diaminobenzoate.

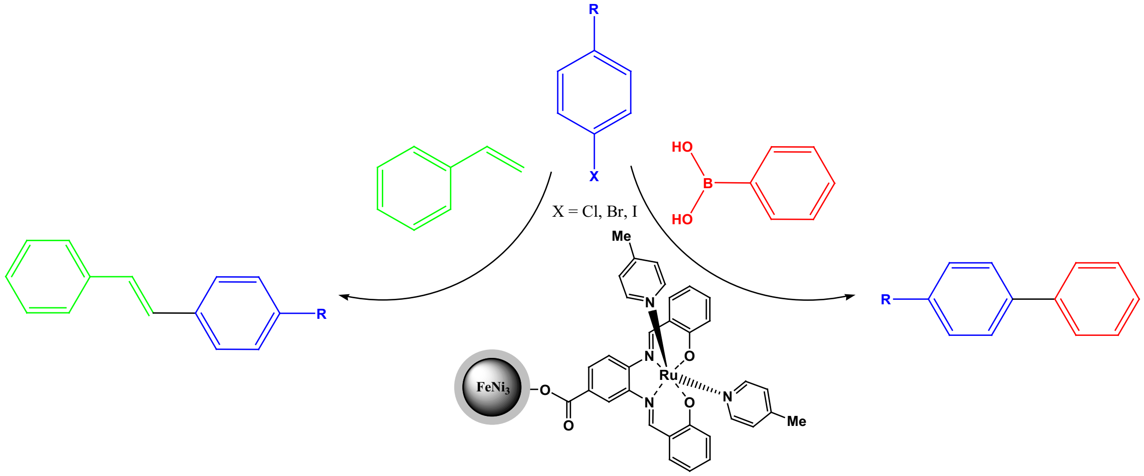

Scheme 1 Heck and Suzuki coupling reactions in the presence of $FeNi_3/SiO_2$/Salen/Ru MNPs

After vigorous stirring for 24 h, the magnetic $FeNi_3/SiO_2$ nanoparticles were collected by magnetic separation and washed with ethanol and deionized water in sequence.

2.5 General Procedure for the Preparation of $FeNi_3/SiO_2$/Salen Nanoparticles

For synthesis of $FeNi_3/SiO_2$/Salen MNPs, Compound (A) (4 g) was suspended in 600 ml of 0.1 M toluene solution of salicylaldehyde and the colloidal solution was refluxed for 24 h. The magnetic $FeNi_3/SiO_2$/Salen nanoparticles were collected by magnetic separation and washed with ethanol and deionized water in sequence (Fig. 1; Table 1).

2.6 General Procedure for the Preparation of $FeNi_3/SiO_2$/Salen/Ru Nanoparticles

A mixture of $FeNi_3/SiO_2$/Salen (0.45 g), $Ru(DMSO)_4Cl_2$ (0.5 g), and Et_3N (0.8 ml) in methanol (10 ml) was degassed with N_2 and refluxed for 4 h. After cooling to room temperature, the precipitate was filtered and washed with methanol (10 × 3 ml) and ether (10 × 3 ml) to get a reddish-brown powder. The powder was mixed with an excess of 4-methylpyridine in methanol (0.5 ml) and heated to reflux for 2 h. The final particle was separated from the solution by applying a magnetic field, washed three times with water to remove any ions present, and dried under vacuum (Fig. 1) [31].

2.7 General Procedure for the Heck Cross-Coupling Reaction

A mixture of arylhalides (1 mmol), styrene (1.2 mmol), K_2CO_3 (3 mmol), and $FeNi_3/SiO_2$/Salen/Ru MNPs (0.1 mg) was stirred at 70 °C in distilled water for an appropriate time. The catalyst was separated by an external magnet, washed with EtOAc, dried and reused for a consecutive run under the same reaction conditions. Evaporation of the solvent of the filtrate under reduced pressure gave the crude products. The pure products were isolated by chromatography on silica gel eluted with *n*-hexane:EtOAc (50:1) (Table 2).

2.8 General Procedure for the Suzuki Cross-Coupling Reaction

A mixture of arylhalides (1 mmol), phenylboronic acid (1.2 mmol), K_2CO_3 (3 mmol), and $FeNi_3/SiO_2$/Salen/Ru MNPs (0.1 mg) was stirred at 50 °C in distilled water for an appropriate time (Table 4). The catalyst was separated by an external magnet, washed with EtOAc, dried and reused for a consecutive run under the same reaction conditions. Evaporation of the solvent of the filtrate under reduced pressure gave the crude products. The pure products were isolated by chromatography on silica gel eluted with *n*-hexane:EtOAc (50:1).

3 Results and Discussion

The first step in the accomplishment of this goal was the synthesis and functionalization of magnetic nanoparticles (Fig. 1). The catalyst was prepared by sonicating nanoferrites with salen (which acts as a robust anchor and avoids Ru) in absolute MeOH, followed by addition of $Ru(DMSO)_4Cl_2$ and 4-methylpyridine. Material with Ru on the functionalized nano-ferrites was obtained in excellent yield. The synthesized $FeNi_3/SiO_2$/Salen/Ru MNP

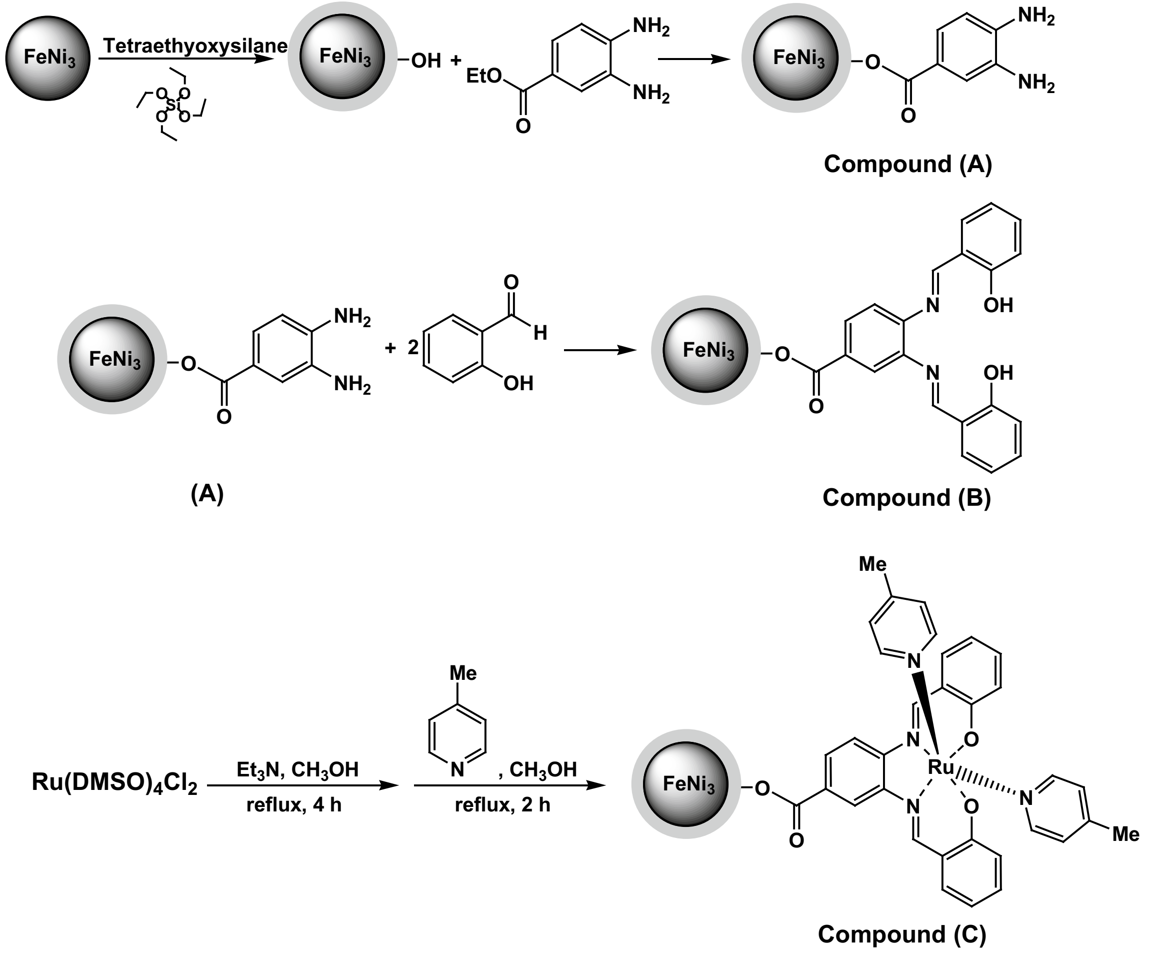

Fig. 1 Schematic illustration of the synthesis for $FeNi_3/SiO_2$/Salen/Ru nanoparticles

Table 1 BET result of $FeNi_3$, and $FeNi_3/SiO_2$/Salen/Ru MNPs

Entry	Catalyst/cycle reusability	Specific surface area (m^2/g)	Pore volume (cm^3/g)	Average pore radius (nm)
1	$FeNi_3$	546	0.802	1.05
2	$FeNi_3/SiO_2$/Salen/Ru	480	0.758	1.88

Calculated by the BJH method

was then characterized by different methods such as N_2 sorption, UV–vis, XRD, TEM, VSM, FTIR, and TGA.

3.1 XRD

The structural properties of synthesized $FeNi_3/SiO_2$/Salen/Ru MNPs was analyzed by X-ray power diffraction (XRD). As shown in Fig. 2, XRD patterns of the synthesized $FeNi_3/SiO_2$/Salen/Ru MNPs display several relatively strong reflection peaks in the 2θ region of 20–80°, which is quite similar to those of $FeNi_3$ nanoparticles reported by other group [32–39]. It can be seen that three characteristic peaks for (FCC)-$FeNi_3$ ($2\theta = 44.3°$, 51.5°, 75.9°) from (111), (200), and (220) planes, are obtained. The sharp and strong diffraction peaks confirm the good crystallization of the products (Fig. 2a). The broad band at $2\theta = 15.0°–30.0°$ can be assigned to the amorphous SiO_2 shell (Fig. 2b) (JCPDS card No. 29–0085).

3.2 FT-IR

Peak appeared at 3120, 2930, 1627, and 1579 cm^{-1} are due to the stretching of the C–H aromatic group, the C–H aliphatic group, C=O group, and C=N group in the $FeNi_3/SiO_2$/Salen/Ru MNPs (Fig. 3a).

3.3 TEM

The size and structure of the $FeNi_3/SiO_2$/Salen/Ru MNPs was also evaluated using transmission electron microscopy

Table 2 The effect of solvent and base in the Heck and Suzuki coupling reaction

Entry	Solvent	Base	Yield (%)[a]	
			Heck	Suzuki
1	–	K_2CO_3	–	–
2	H_2O	K_2CO_3	97	95
3	MeOH	K_2CO_3	73	81
4	EtOH	K_2CO_3	89	82
5	Toluene	K_2CO_3	14	–
6	CH_3CN	K_2CO_3	16	–
7	DMF	K_2CO_3	21	28
8	THF	K_2CO_3	11	19
9	H_2O	Na_2CO_3	91	78
10	H_2O	Et_3N	69	59
11	H_2O	NaOAc	32	45
12	H_2O	KOH	61	37
13	H_2O	K_3PO_4	34	61
14	H_2O	Cs_2CO_3	57	23
15	H_2O	*t*BuOK	48	32

Reaction conditions bromobenzene (1 mmol), phenylboronic acid or styrene (1.2 mmol), base (3 mmol), catalyst (0.2 mg), solvent (3 ml), 100 °C, 2.5 h

[a] GC yields [%]

Table 3 Influence of different catalysts for Heck and Suzuki coupling reaction

Entry	Catalyst	Yield (%)[a]	
		Heck	Suzuki
1	$FeNi_3$	–	–
2	$FeNi_3/SiO_2$	–	–
3	$FeNi_3/SiO_2$/Salen	17	11
4	$FeNi_3/SiO_2$/Salen/Ru	97	95
5	Salen/Ru	95	96

Reaction conditions (a) Heck coupling reaction: bromobenzene (1 mmol), styrene (1.2 mmol), catalyst (0.1 mg), K_2CO_3 (3 mmol), H_2O (3 ml), 70 °C; (b) Suzuki coupling reaction: bromobenzene (1 mmol), phenylboronic acid (1.2 mmol), catalyst (0.1 mg), K_2CO_3 (3 mmol), H_2O (3 ml), 50 °C

[a] Isolated yield

(TEM) (Fig. 4). The average size of $FeNi_3$ MNPs is about 10–15 nm (Fig. 4a). After being coated with a silica layer, the typical core–shell structure of the $FeNi_3/SiO_2$ MNPs can be observed. The dispersity of $FeNi_3/SiO_2$ MNPs is also improved, and the average size increases to about 15–20 nm (Fig. 4b). The TEM image of the $FeNi_3/SiO_2$/Salen/Ru MNPs are shown in Fig. 4c. The functionalization of the $FeNi_3/SiO_2$/Salen/Ru MNPs does not result in the change of the morphology. The average size of $FeNi_3/SiO_2$/Salen/Ru MNPs is about 30–45 nm.

Table 4 Heck cross-coupling of various arylhalides with styrene in the presence of $FeNi_3/SiO_2$/Salen/Ru MNP catalyst in water

Entry	Arylhalide	Time (h)	Yield (%)[a]
1	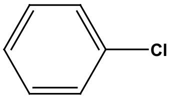	7	88
2	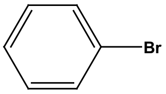	1	97
3	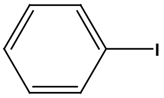	1	97
4	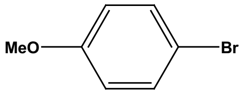	0.5	95
5	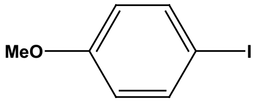	0.5	>99
6	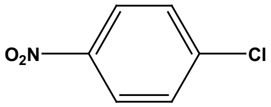	9	92
7	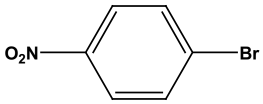	0.5	96

Reaction conditions arylhalide (1 mmol), styrene (1.2 mmol), catalyst (0.1 mg), K_2CO_3 (3 mmol), H_2O (3 ml), 70 °C

[a] Isolated yields (%)

3.4 Thermo-Gravimetric Analysis (TGA)

The thermal behavior of $FeNi_3/SiO_2$/Salen/Ru MNPs is shown in Fig. 5. A significant decrease in the weight percentage of the $FeNi_3/SiO_2$/Salen/Ru MNPs at about 130 °C is related to desorption of water molecules from the catalyst surface. This was evaluated to be 1–3 % according to the TG analysis. In addition, the analysis showed two other decreasing peaks. First peak appears at temperature around 250–280 °C due to the decomposition of Ru. This is followed by a second peak at 420–460 °C, corresponding to the loss of the organic spacer group. These results were in agreement with those obtained by ICP. The ICP analysis showed that 0.61 mmol of ruthenium was anchored on 0.9 g of MNPs.

3.5 Magnetic Properties of the $FeNi_3/SiO_2$/Salen/Ru MNPs

The magnetic properties of the nanoparticles were characterized using a vibrating sample magnetometer (VSM).

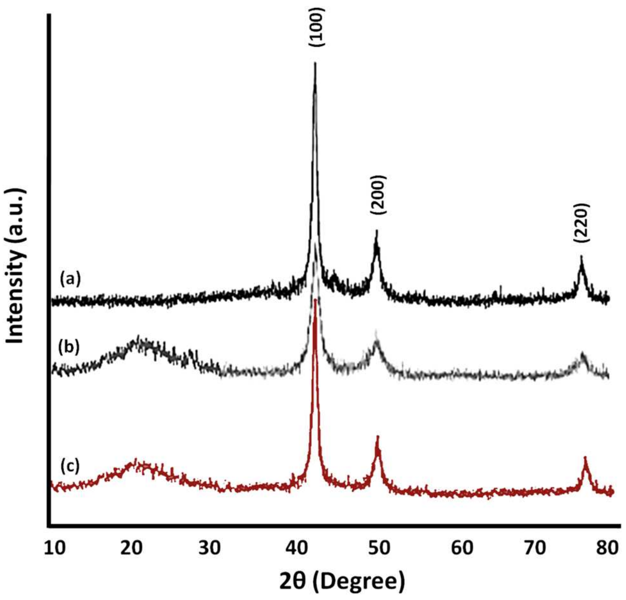

Fig. 2 XRD analysis of **a** $FeNi_3$, and **b** $FeNi_3/SiO_2$/Salen/Ru, **c** recovered $FeNi_3/SiO_2$/Salen/Ru MNPs

The magnetization curves of the obtained nanocomposite registered at 300 K show nearly no residual magnetism is detected (Fig. 6), which means that the nanocomposite exhibited the paramagnetic characteristics. Magnetic measurement shows that pure $FeNi_3$, and $FeNi_3/SiO_2$/Salen/Ru have saturation magnetization values of 50.2, and 23.4 emu/g respectively. These nanocomposites with paramagnetic characteristics and high magnetization values can quickly respond to the external magnetic field and quickly redisperse once the external magnetic field is removed. The result reveals that the nanocomposite exhibit good magnetic responsible, which suggests a potential application for targeting and separation.

3.6 UV–Vis Spectroscopy

The UV–vis spectra of neat complex and the supported Ru(II) catalysts are given in Fig. 7. The spectra of the supported ruthenium catalysts showed features similar to those of the neat complex. The bands at 210 and 325 nm can be attributed to the charge transfer transition of salen ligand. The band at 475 nm is due to ligand-to-metal charge transfer transition of Ru(II) salen complex. On immobilization of Ru salen complex, all the characteristic bands appeared in its spectra. The UV–vis spectra confirmed the immobilization of Ru salen complex on the supports.

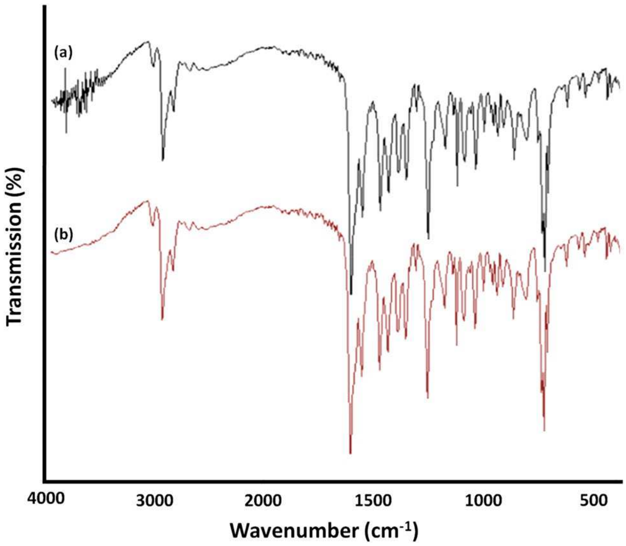

Fig. 3 FTIR spectra of **a** fresh $FeNi_3/SiO_2$/Salen/Ru MNPs, **b** recovered $FeNi_3/SiO_2$/Salen/Ru MNPs

3.7 N_2 Sorption Study

N_2 adsorption measurements, which have been a powerful tool for nano- or mesoporous material characterization, were performed to attain more insights into the modified $FeNi_3$. The samples displayed a type IV isotherm (as defined by IUPAC) with H_1 hysteresis and a sharp increase in pore volume adsorbed above P/P_0 0.7–0.8 cm^3/g, which is a characteristic of highly ordered mesoporous materials. The textural properties of $FeNi_3$ were substantially maintained over ruthenium complexation with salen complex. A sharp decrease in surface areawas observed for $FeNi_3$ and $FeNi_3/SiO_2$/Salen/Ru MNPs from 546 to 480 m^2/g, respectively, and the average pore volume decreased from 0.802 to 0.758 cm^3/g (Table 1). The average pore diameters also decreased from 1.05 to 1.88 nm. This suggests that the Ru–salen complex may be well confined in the pores of the $FeNi_3$.

3.8 Catalytic Activity of $FeNi_3/SiO_2$/Salen/Ru MNPs for Heck and Suzuki Coupling

The efficiency of $FeNi_3/SiO_2$/Salen/Ru MNPs is significantly affected by the type of solvent and base used in the reactions (Table 2). The reactions were do better in protic solvent (Table 2, entry 2–4). On the other hand, remarkably high activity wasre producibly found in water (entry 2). The ability to use water as the reaction medium greatly increases the green credentials of the method. Among the

Fig. 4 **a** TEM images of $FeNi_3$ MNPs, **b** $FeNi_3/SiO_2$ MNPs, **c** $FeNi_3/SiO_2$/Salen/Ru MNPs, **d** $FeNi_3/SiO_2$/Salen/Ru MNPs after ten reuses

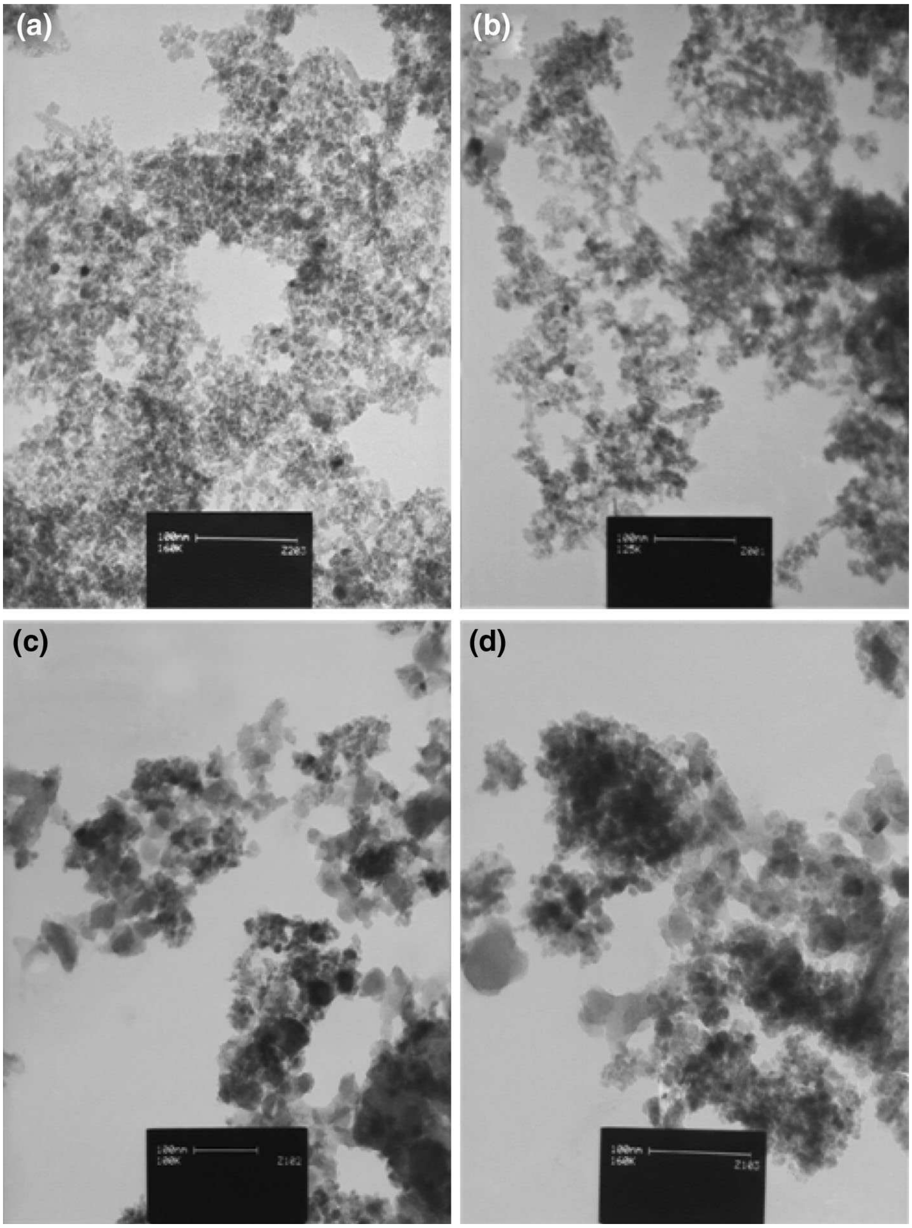

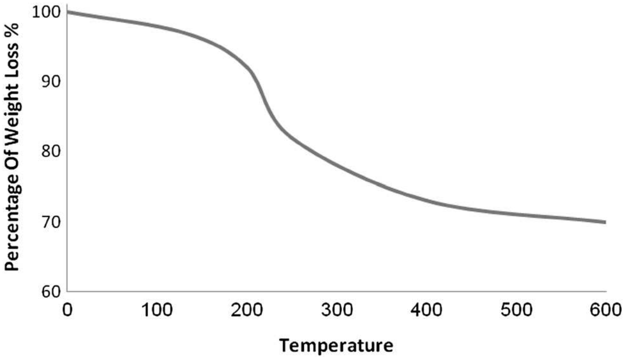

Fig. 5 TGA diagram of nano catalysis

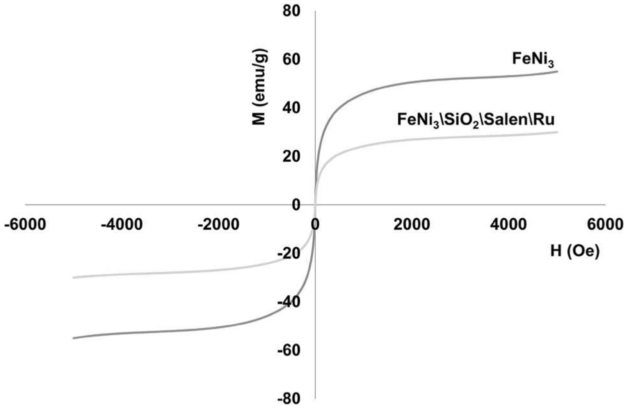

Fig. 6 Room-temperature magnetization curves of the nano catalysis

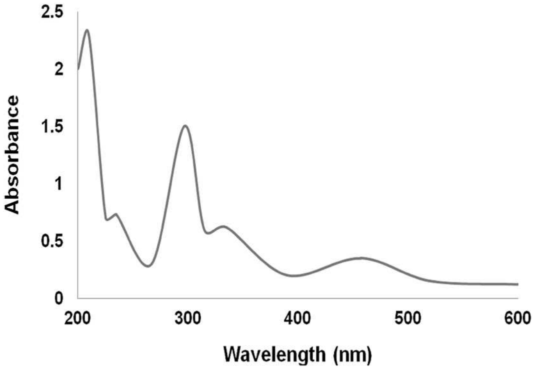

Fig. 7 UV–vis of catalyst

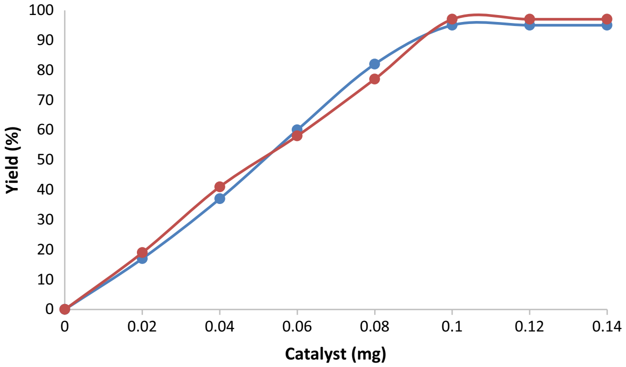

Fig. 8 Effect of amount of the catalyst on yield of products. *Red*: Heck, and *blue*: Suzuki coupling reaction

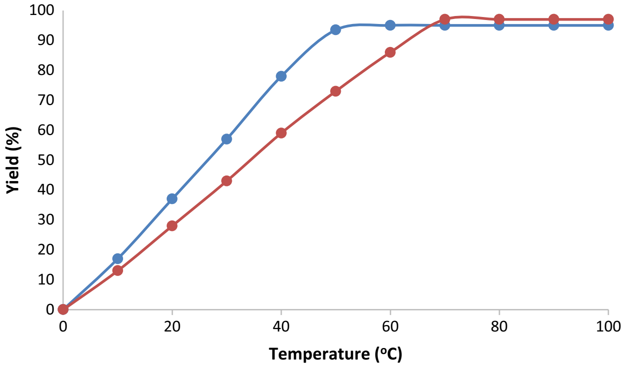

Fig. 9 Effect of temperature on yield of products. *Red*: Heck, and *blue*: Suzuki coupling reaction

Table 5 Suzuki cross-coupling of various arylhalides with phenylboronic acid in the presence of $FeNi_3/SiO_2$/Salen/Ru MNP catalyst in water

Entry	R	Time (h)	Yield (%)[a]
1	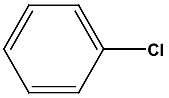	7	87
2	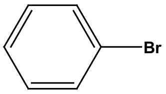	1	95
3	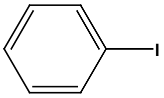	1	96
4	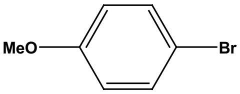	0.5	94
5	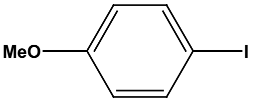	0.5	>99
6	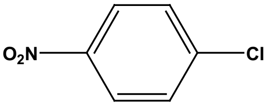	9	91
7	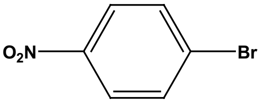	0.5	94

Reaction conditions: arylhalide (1 mmol), phenylboronic acid (1.2 mmol), catalyst (0.1 mg), K_2CO_3 (3 mmol), H_2O (3 ml), 50 °C

[a] Isolated yields (%)

studied bases, K_2CO_3 showed the best results for this reaction in terms of reaction time and yield (Table 2, entrie 2).

At this stage, the amount of catalyst necessary to promote the reactions efficiently was examined. It was observed that the variation for $FeNi_3/SiO_2$/Salen/Ru MNP had an effective influence. The best amount of $FeNi_3/SiO_2$/Salen/Ru MNP is 0.1 mg for both of Heck and Suzuki coupling reaction (Fig. 8). We also investigated the crucial role of temperature in the Heck and Suzuki coupling reaction in the presence of $FeNi_3/SiO_2$/Salen/RuMNPs as a catalyst. Results clearly indicated that the catalytic activity is sensitive to reaction temperature. The best temperature for Heck coupling was 70 °C and for Suzuki coupling was 50 °C. Temperatures greater than the resulting temperatures does not cause changes in the efficiency of the reaction (Fig. 9).

To further evaluate the efficiency of the catalyst, different control experiments were performed and the obtained data is shown in Table 3. Initially, a standard reaction was carried out using $FeNi_3$ and $FeNi_3/SiO_2$, no product formation was observed. The result of this studies showed that any amount of the desired product was not formed (Table 3, entries 1 and 2). When $FeNi_3/SiO_2$/Salen was used as the catalyst, a reaction was observed, although the yield of the desired product was very low (Table 3, entries 3). The Salen could not give the satisfactory catalytic activity under mild reactions. Based on these frustrating results, we continued the research to improve the yield of the product by added the Ru

Table 6 Comparison of the catalytic efficiency of $FeNi_3/SiO_2$/Salen/Ru MNPs with various catalysts

Entry	Coupling reaction	Catalyst	Base	Solvent	Temperature (°C)	Time (h)	Yield (%)	Ref.
1	Heck	TiO_2@Pd nanoparticles	Et_3N	DMF	140	24	91	[40]
2	Heck	'Si'–2As–Pd(0)	Bu_3N	*p*-Xylene	140	12	52	[41]
3	Heck	Fluorous palladium catalyst	K_2CO_3	H_2O	100	24	73	[21]
4	Heck	Pd/Fe_3O_4	K_2CO_3	NMP	130	12	67.3	[42]
5	Heck	Pd–SBA	Et_3N	–	170	48	85	[43]
6	Heck		Bu_3N	NMP	130	18	81	[44]
7	Heck	Pd–TPA/ZrO_2	K_2CO_3	DMF	120	6	59	[45]
8	Heck	MCM-41-SH-Pd(0)	Bu_3N	NMP	130	18	80	[46]
9	Heck	Au/Pd NPs	K_2CO_3	H_2O	80	12	85	[47]
10	Heck	POCOP[a]	K_2CO_3	DMF	100	6	85	[48]
11	Heck	$[Pd(L)Cl_2]$[b]	K_2CO_3	DMF	110	24	75	[49]
12	Heck	Pd-DABCO-γ-Fe_2O_3	Et_3N	–	100	7	83	[50]
13	Heck	γ-Fe_2O_3-acetamidine-Pd	Et_3N	DMF	100	0.5	69	[51]
14	Heck	Pd-isatin Schiff base-γ-Fe_2O_3	Et_3N	–	100	7	63	[52]
15	Heck	$FeNi_3/SiO_2$/Salen/Ru	K_2CO_3	H_2O	70	1	97	This work
16	Suzuki	SiO_2-*p*A-Cyan-*Cys*-Pd[c]	K_2CO_3	H_2O	100	5.5	88	[53]
17	Suzuki	NHC–Pd(II) complex[d]	$K_3PO_4{\cdot}3H_2O$	H_2O	40	6	90	[54]
18	Suzuki	Bis(oxamato)palladate(II)complex[e]	Et_3N	*n*-Bu_4NBr	120	2	65	[55]
19	Suzuki	Pd_3(dba) [f]	K_3PO_4	THF	80	24	78	[56]
20	Suzuki	Pd-isatin Schiff base-γ-Fe_2O_3	Et_3N	–	100	0.75	90	[52]
21	Suzuki	$FeNi_3/SiO_2$/Salen/Ru	K_2CO_3	H_2O	50	1	95	This work

[a] POCOP: Bisphosphinite PCP-pincer palladium complex

[b] L: 1-benzyl-4-phenylthiomethyl

[c] SiO_2-*p*A-Cyan-*Cys*-Pd: Propylamine-cyanuric-cysteine palladium complex immobilized onto silica

[d] NHC-Pd (II): [1,1-(hexylene-1,6-diyl)bis(3-*n*-butylbenzimidazol-2-ylidene)]$[PdCl_2(CH_3CN)]_2$

[e] Bis(oxamato)palladate(II) complexes: $(n\text{-}Bu_4N)_2[Pd(2\text{-}Mepma)_2].4H_2O$

[f] Pd_3(dba): $N_3P_3(O\text{–}C_6H_4\text{-}p\text{-}P(C_6H_5)_2)_5(O\text{–}C_6H_4\text{-}p\text{-}C_6H_4\text{-}p\text{–}O(CH_2)_3Si(OCH_3)_3$

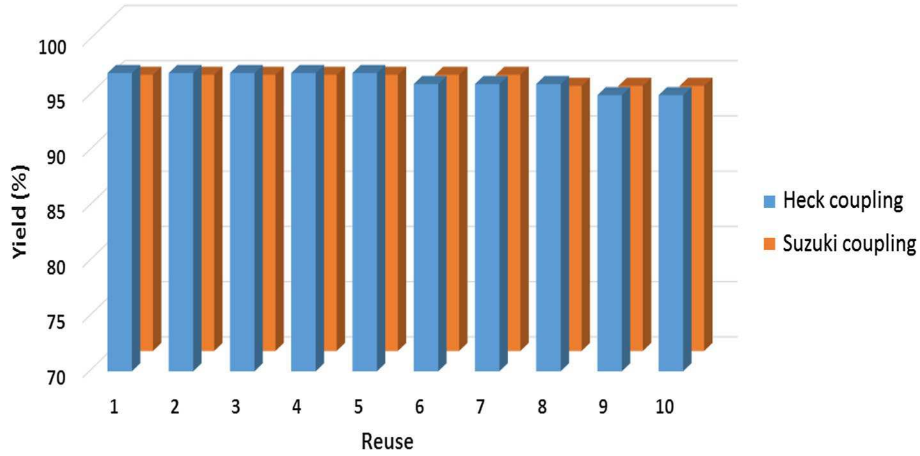

Fig. 10 Reuses performance of the catalysts

(II) to catalyst. Notably, there was not much difference in the reaction yields when reaction was carried out using $FeNi_3/SiO_2$/Salen/Ru MNP and Salen/Ru catalyst (Table 3, entries 4 and 5). The nano-sized particles increase the exposed surface area of the active site of the catalyst, thereby enhancing the contact between reactants and catalyst dramatically and mimicking the homogeneous catalysts. Also, the activity and selectivity of nano-catalyst can be manipulated by tailoring chemical and physical properties like size, shape, composition and morphology. As a result, $FeNi_3/SiO_2$/Salen/Ru MNP was used in the subsequent investigations because of its high reactivity, high selectivity and easy separation by using the magnetic properties of $FeNi_3$.

Then, the reaction of a various types of iodo-, bromo-, and chloroaryl derivatives with styrene in the presence $FeNi_3/SiO_2$/Salen/Ru MNP (0.1 mg) and K_2CO_3 at 70 °C in water as solvent was investigated. The results of this study are collected in Table 4. To demonstrate the scope of the catalyst system, aryl halides including chlorides, bromides and iodides with various substitutions were cross coupled with styrene ethyl and methyl acrylates to give good to high yields of the products irrespective of the nature of substituents like nitro, and methoxy groups.

Following this initial success in the Suzuki cross-coupling reaction, we investigated the application of $FeNi_3/SiO_2$/Salen/Ru MNP in the Suzuki reaction. As shown in Table 5, various aryl iodides, bromides and chlorides containing electron-donating and electron-withdrawing groups underwent the cross-coupling reaction with phenylboronic acid to produce the corresponding products in good to high yields.

To show the advantages of proposed method in comparison with other reported methods, we summarized some of results for Heck and Suzuki coupling reaction of styrene with bromobenzene in Table 6, which shows that $FeNi_3/SiO_2$/Salen/Ru is an equally or more efficient catalyst with respect to reaction time and yield than previously reported ones.

It is important to note that the magnetic property of $FeNi_3/SiO_2$/Salen/Ru MNPs facilitates its efficient recovery from the reaction mixture during work-up procedure. The activity of the recycled catalyst was also examined under the optimized conditions. After the completion of reaction, The catalyst was separated by an external magnet, washed with methanol and dried at the pump. The recovered catalyst was reused for ten consecutive cycles without any significant loss in catalytic activity (Fig. 10). The recyclablity test was stopped after ten runs. Comparison of TEM images (Fig. 4d), FT-IR spectra (Fig. 3b), and XRD patterns (Fig. 2c) of used catalyst with those of the fresh catalyst (Figs. 2b, 3a, 4c,) showed that the morphology and structure of $FeNi_3/SiO_2$/Salen/Ru MNPs remained intact after ten recoveries. In order to know whether the reaction takes place at the surface of $FeNi_3/SiO_2$/Salen/Ru MNPs as a truly heterogeneous catalyst any Ru(II) species as a homogeneous catalyst, ICP analysis of the remaining mixture after catalyst and product separation was investigated upon reaction completion. The amount of Ru(II) leaching after the ten repeated recycling was 3.5 %. These observations indicated that the catalyst was stable and could tolerate the present reaction conditions.

4 Conclusion

In summary, $FeNi_3/SiO_2$/Salen/Ru MNP as a new magnetic nanoparticles catalyst was synthesized directly through reaction of $Ru(DMSO)_4Cl_2$ and 4-methylpyridine complex supported on $FeNi_3/SiO_2$/SalenMNP. The synthesized $FeNi_3/SiO_2$/Salen/Ru MNP was used as a magnetically recyclable heterogeneous catalyst for the efficient one-pot synthesis of Heck and Suzuki coupling reactions with high product yields. The catalytic research on novel approaches toward nanomaterials should be improved to enhance organic synthesis. For that purpose, nanoparticles catalyst provides a new way for continuous processes, because of its simple recyclability. From a scientific point, our results expand the application of nanoparticles. This catalyst should be helpful to development of new catalytic systems.

References

1. Zheng X, Luo S, Zhang L, Cheng JP (2009) Green Chem 11:455
2. Jiang Y, Guo C, Xia H, Mahmood I, Liu C, Liu H (2009) J Mol Catal B 58:103
3. Sadeghzadeh SM (2014) ChemPlusChem 79:278
4. Sadeghzadeh SM, Daneshfar F (2014) J Mol Liq 199:440
5. Sadeghzadeh SM, Nasseri MA (2014) J Iran Chem Soc 11:1197
6. Gottschalk F, Nowack B (2011) J Environ Monit 13:1145
7. Zhu M, Nie G, Meng H, Xia T, Nel A, Zhao Y (2013) Acc Chem Res 46:622
8. Braga M, Quecchia C, Perotta C, Timpini A, Maccarinelli K, Di Tommaso L, Di Gioacchino M (2013) Int J Immunopathol Pharmacol 26:707
9. Gornati R, Pedretti E, Rossi F, Cappellini F, Zanella M, Olivato I, Sabbioni E, Bernardini G (2016) J Appl Toxicol 36:385
10. Beller M, Bolm C (2004) Transition metals for organic synthesis: building blocks and fine chemicals, 2nd edn. Wiley VCH, Weinheim
11. Brennfhrer A, Neumann H, Beller M (2009) Angew Chem Int Ed 48:4114
12. Vries AH, Mulders JMCA, Mommers JHM, Henderickx HJW, Vries JG (2003) Org Lett 5:3285
13. Chinchilla R, Njera C (2007) Chem Rev 107:874
14. Heck RH (1985) Palladium reagents for organic synthesis. Academic Press, New York
15. Allred GD, Liebeskind LS (1996) J Am Chem Soc 118:2748
16. Zhang ZY, Hu HW, Kao TY (1990) React Polym Ion Exch Sorbents 12:229
17. Bergmann F, Schapira D (1947) J Org Chem 12:57
18. Kamal A, Srinivasulu V, Seshadri BN, Markandeya N, Alarifi A, Shankaraiah N (2012) Green Chem 14:2513.
19. Niknam K, Sadeghi Habibabad M, Deris A, Panahi F, Hormozi Nezhad MR (2013) J Iran Chem Soc 10:527
20. Cui X, Li Z, Tao CZ, Xu Y, Li J, Liu L, Guo QX (2006) Org Lett 8:2467.
21. Wan L, Cai C (2011) Transition Met Chem 36:747
22. Sadeghzadeh SM (2014) RSC Adv 4:43315
23. Sadeghzadeh SM, Daneshfar F (2016) J Mol Catal A 423:216
24. Sadeghzadeh SM, Nasseri MA (2013) Catal Today 217:80
25. Sadeghzadeh SM (2015) Green Chem 17:3059
26. Sadeghzadeh SM, Daneshfar F, Malekzadeh M (2014) Chin J Chem 32:349

27. Sadeghzadeh SM, Malekzadeh M (2015) J Mol Liq 202:46
28. Primerano P, Milazzo MF, Risitano F, Cordaro M, Scala A (2016) J Ind Eng Chem. doi:10.1016/j.jiec.2016.07.042
29. Primerano P, Milazzo MF, Risitano F, Matarazzo A (2016) J Chem Technol Biotechnol 91(5):1274
30. Qiu T, Guo X, Yang J, Zhou L, Li L, Wang H, Niu Y (2016) Chem Eng J 296:71
31. Jiang Y, Li F, Huang F, Zhang B, Sun L (2013) Chinese J Catal 34:1489
32. Ma T, Yuan M, Islam SM, Li H, Ma S, Sun G, Yang X (2016) J Alloy Compd 678:468
33. Ding X, Huang Y, Zong M (2015) Mater Lett 157:285
34. Bac LH, Kwon YS, Kim JS, Lee YI, Lee DW, Kim JC (2010) Mater Res Bull 45:352
35. Lu X, Huo G, Liu X, Liang G, Han Z, Song X (2012) Cryst Eng Commun 14:5622
36. Fu LS, Jiang JT, Zhen L, Shao WZ (2013) Mater Sci Eng B 178:225
37. Sun Y, Liu X, Feng C, Fan J, Lv Y, Wang Y, Li C (2014) J Alloy Compd 586:688
38. Lu X, Wu J, Huo G, Sun Q, Huang Y, Han Z, Liang G (2012) Colloids Surf A 414:168
39. Chen YC, Zheng FC, Min YL, Wang T, Zhao YG (2012) Solid State Sci 14:809
40. Nasrollahzadeh M, Azarian A, Ehsani A, Khalaj M (2014) J Mol Catal A 394:205
41. Cai M, Huang Y, Zhao H, Song C (2003) J Organomet Chem 682:20
42. Zhang F, Niu J, Wang H, Yang H, Jin J, Liu N, Zhang Y, Li R, Ma J (2012) Mat Res Bull 47:504
43. Li L, Shi JL, Yan JN (2004) Chem Commun 1990
44. Cai M, Xu Q, Jiang J (2006) J Mol Catal A 260:190
45. Pathan S, Patel A (2012) RSC Adv 2:116
46. Xu Q, Cai M (2007) React Funct Polym 67:515
47. Nasrollahzadeh M, Banaei A (2015) Tetrahedron Lett 56:500
48. Tamami B, Nezhad MM, Ghasemi S, Farjadian F (2013) J Organomet Chem 743:10
49. Saleem F, Rao GK, Kumar A, Kumar S, Singha M P, Singh A K (2014) RSC Adv 4:56102
50. Sobhani S, Pakdin-Parizi Z (2014) Appl Catal A 479:112
51. Sobhani S, Ghasemzadeh MS, Honarmand M, Zarifi F (2014) RSC Adv 4:44166.
52. Sobhani S, Zarifi F (2015) Chinese J Catal 36:555
53. Ghiaci M, Zargani M, Moeinpour F, khojastehnezhad A (2014) Appl Organomet Chem 28:589
54. Liu QX, Zhang W, Zhao XJ, Zhao ZX, Shi MC, Wang XG (2013) Eur J Org Chem 2013:1253
55. Fortea-Pérez FR, Schlegel I, Julve M, Armentano D, De Munno G, Stiriba SE (2013) J Organomet Chem 743:102
56. de Paula VI, Sato CA, Buffon R (2012) J Braz Chem Soc 23:258.